

Tensor Field Segmentation Using Region Based Active Contour Model*

Zhizhou Wang and Baba C. Vemuri

Department of CISE, University of Florida
Gainesville, Fl. 32611
{zwang,vemuri}@cise.ufl.edu

Abstract. Tensor fields (matrix valued data sets) have recently attracted increased attention in the fields of image processing, computer vision, visualization and medical imaging. Tensor field segmentation is an important problem in tensor field analysis and has not been addressed adequately in the past. In this paper, we present an effective region-based active contour model for tensor field segmentation and show its application to diffusion tensor magnetic resonance images (MRI) as well as for the texture segmentation problem in computer vision. Specifically, we present a variational principle for an active contour using the Euclidean difference of tensors as a discriminant. The variational formulation is valid for piecewise smooth regions, however, for the sake of simplicity of exposition, we present the piecewise constant region model in detail. This variational principle is a generalization of the region-based active contour to matrix valued functions. It naturally leads to a curve evolution equation for tensor field segmentation, which is subsequently expressed in a level set framework and solved numerically. Synthetic and real data experiments involving the segmentation of diffusion tensor MRI as well as structure tensors obtained from real texture data are shown to depict the performance of the proposed model.

1 Introduction

Tensor fields are the essential components in many applications like DT-MRI processing, texture image segmentation, solid and fluid mechanics etc. Several interesting problems constitute tensor field analysis in the context of imaging applications, for example : tensor field data acquisition, restoration, segmentation and visualization. Though, much effort has been expended on tensor field data acquisition, restoration and visualization, tensor field segmentation has not been adequately addressed in the past. In this paper, we will address the general problem of tensor field segmentation and then depict examples of application of the algorithm to medical image analysis, specifically to diffusion tensor MRI segmentation and additionally to texture image segmentation. In the following, we will present a brief overview of various techniques currently invogue in using tensor-based information for segmenting motion fields, textures and DT-MRI.

* This research was in part funded by the NIH grant RO1-NS42075

There are many algorithms in literature for motion segmentation, however, not many of them use the structure tensor. Kühne et.al [11] proposed an interesting tensor-driven active contour model for moving object segmentation, a 3D structure tensor is computed in the spatio-temporal domain of a video sequence and is used to create the stopping function in a geometric active contour model. The results they shown are quite promising for motion segmentation. Some other examples of published research on the use of the structure tensor in the context of optical flow computation are [4,9].

Recently, Rousson et.al, in [12] developed a technique for segmenting textures where in they first construct texture features based on the image and its structure tensor, then use an active and adaptive contour model to segment this feature vector field. The texture segmentation results are very impressive in their work.

In the context of DT-MRI segmentation, recently, Zhukov et.al., [18] proposed a level set segmentation method which is in fact a segmentation of a scalar anisotropic measure of the diffusion tensor. The fact that Zukhov et.al., [18] use a scalar field computed from the diffusion tensor field implies they have ignored the direction information contained in the tensor field. Thus, this method will fail if two homogeneous regions of tensor field have the same anisotropy property but are oriented in a totally different direction! Moreover, any of the numerous (well tested and well understood) scalar image segmentation techniques could have been employed for achieving the goal of segmenting the scalar field of anisotropy measures. In contrast, we present an algorithm to segment tensor field using all the information contained in a tensor, not only scalar anisotropy properties, but also its orientation.

To the best of our knowledge, there is no published work in literature which aims to segment tensor fields. In this paper, we tackle the tensor field segmentation problem using an effective region based active contour model. Geometric active contour model has long been used in scalar and vector images segmentation [5,6,13,14,10,17]. Our work can be viewed as an *extension* of the work on the region-based active contours ([7],[8], [17]), *to matrix valued images*. These region-based active contours are curve evolution implementation of the Mumford-Shah functional [15]. *Our key contribution is the incorporation of a discriminant of tensors into the region based active contour model and to show its effectiveness in tensor field segmentation*. The specific discriminant we use is the Forbenius norm of the difference of two tensors. Although this norm has been used in the past for tensor field restoration, to the best of our knowledge, it has never been used for tensor field segmentation.

Rest of the paper is organized as follows: in section 2, the piecewise smooth and piecewise constant region-based active contour models for tensor field segmentation are described. The Euler-Lagrange equation and the curve evolution equation are given for the piecewise constant model for simplicity of exposition. Section 3 contains a detailed description of the level set formulation and the implementation using an explicit scheme. In section 4, we present experiments on application of our model to synthetic as well as real data. Finally in section 5, we discuss the pros and cons of our approach and some future directions.

2 Model Description

Our model for tensor field segmentation in R^2 is posed as minimization of the following variational principle based on the Mumford-Shah functional ([15]):

$$E(\mathbf{T}, \mathbf{C}) = \int_{\Omega} dist(\mathbf{T}(\mathbf{x}), \mathbf{T}_0(\mathbf{x}))^2 d\mathbf{x} + \alpha \int_{\Omega/C} \|\nabla \mathbf{T}(\mathbf{x})\|^2 d\mathbf{x} + \beta |\mathbf{C}| \quad (1)$$

Where the curve \mathbf{C} is the boundary of the desired unknown segmentation, Ω is the image domain, \mathbf{T}_0 is the original noisy tensor field, \mathbf{T} is a piecewise smooth approximation of \mathbf{T}_0 with discontinuities only along \mathbf{C} , $\nabla \mathbf{T}$ is a component wise gradient of each element of the tensor, $|\mathbf{C}|$ is the arclength of the curve \mathbf{C} , α and β are control parameters, $dist(., .)$ is a measure of the distance between two tensors.

The above variational principle will capture piecewise smooth regions while maintaining a smooth boundary. A simplified form which aims to capture two types of piecewise constant regions is given by:

$$E(C, \mathbf{T}_1, \mathbf{T}_2) = \int_R dist^2(\mathbf{T}(\mathbf{x}), \mathbf{T}_1) d\mathbf{x} + \int_{R^c} dist^2(\mathbf{T}(\mathbf{x}), \mathbf{T}_2) d\mathbf{x} + \beta |C| \quad (2)$$

where R is the region enclosed by C and R^c is the region outside C .

The above model in equation (2) can be viewed as a modification of the active contour model without edges for scalar valued images in [7]. The difference measures in [7] for the scalar values are simple, be it intensity or curvature. In the proposed model, a key issue will be the right choice of a tensor difference measure. Any other segmentation models that are generalizations of the one proposed here for tensor fields, will unavoidably encounter this fundamental problem. Alexander et.al., [1] discussed different similarity measures for matching of diffusion tensor images and indicated that the Euclidean difference measure of tensors is the best in the context of image registration. The Euclidean difference metric is defined as follows:

$$dist(A, B) = \sqrt{trace[(A - B)^2]} = \|A - B\|_F \quad (3)$$

where A and B are two rank 2 tensor of the same size, or simply two matrices of the same size, $\|\cdot\|_F$ is the matrix Frobenius Norm.

In the context of tensor field segmentation, we also found that the Euclidean difference measure of tensors is a good choice. We define the mean value of tensors in a region R as:

$$\mu(\mathbf{T}; R) = \min_{\mu} \int_R [dist(\mu, \mathbf{T}(\mathbf{x}))]^2 d\mathbf{x} \quad (4)$$

When we choose $dist(., .)$ to be the Euclidean difference measure, it is not hard to verify that $\mu(\mathbf{T}) = \int_R \mathbf{T}(\mathbf{x}) d\mathbf{x} / |R|$.

We followed the two phases implementation of ([7]). First fixed \mathbf{C} , then $\mathbf{T}_1 = \mu(\mathbf{T}; R)$ and $\mathbf{T}_2 = \mu(\mathbf{T}; R^c)$. Then fixed \mathbf{T}_1 and \mathbf{T}_2 , the Euler Lagrange equation for the variational principle (2) is:

$$[\beta k - dist^2(\mathbf{T}, \mathbf{T}_1) + dist^2(\mathbf{T}, \mathbf{T}_2)] \mathbf{N} = 0$$

where \mathbf{N} is the outer normal of the curve C . We then have the corresponding gradient flow or the curve evolution form for the above equation as:

$$\begin{aligned} \frac{\partial C}{\partial t} &= - [\beta k - \text{dist}^2(\mathbf{T}, \mathbf{T}_1(t)) + \text{dist}^2(\mathbf{T}, \mathbf{T}_2(t))] \mathbf{N} \\ \mathbf{T}_1 &= \frac{\int_R \mathbf{T}(\mathbf{x}) d\mathbf{x}}{|R|}, \quad \mathbf{T}_2 = \frac{\int_{R^c} \mathbf{T}(\mathbf{x}) d\mathbf{x}}{|R^c|} \end{aligned} \quad (5)$$

This can be easily solved numerically as described subsequently. In a similar fashion, one can write down the curve evolution equation for equation (1).

3 Level Set Implementation and Numerical Methods

The curve evolution equation (5) can be easily implemented in a level set framework. The corresponding level set formulation is given by:

$$\begin{aligned} \frac{\partial \phi}{\partial t} &= \left[\beta \text{div} \left(\frac{\nabla \phi}{|\nabla \phi|} \right) - \text{dist}^2(T, T_1) + \text{dist}^2(T, T_2) \right] |\nabla \phi| \\ T_1 &= \frac{\int_{\Omega} (1 - H(\phi)) T(\mathbf{x}) d\mathbf{x}}{\int_{\Omega} (1 - H(\phi)) d\mathbf{x}}, \quad T_2 = \frac{\int_{\Omega} H(\phi) T(\mathbf{x}) d\mathbf{x}}{\int_{\Omega} H(\phi) d\mathbf{x}} \end{aligned} \quad (6)$$

where $H(\cdot)$ is the Heaviside function, $H(\phi(\mathbf{x})) = 0$ for $x \in R$ and $H(\phi(\mathbf{x})) = 1$ otherwise. Equation (6) can be easily discretized using an explicit Euler scheme. We can assume the spatial grid size to be 1, then the finite differences of the partial derivatives are:

$$\begin{aligned} \Delta^i \phi_{i,j} &= \frac{1}{2} (\phi_{i+1,j} - \phi_{i-1,j}), \quad \Delta^j \phi_{i,j} = \frac{1}{2} (\phi_{i,j+1} - \phi_{i,j-1}) \\ \Delta_-^i \phi_{i,j} &= \phi_{i,j} - \phi_{i-1,j}, \quad \Delta_-^j \phi_{i,j} = \phi_{i,j} - \phi_{i,j-1} \\ \Delta_+^i \phi_{i,j} &= \phi_{i+1,j} - \phi_{i,j}, \quad \Delta_+^j \phi_{i,j} = \phi_{i,j+1} - \phi_{i,j} \\ \Delta^{ii} \phi_{i,j} &= \phi_{i+1,j} - 2\phi_{i,j} + \phi_{i-1,j} \\ \Delta^{ij} \phi_{i,j} &= \frac{1}{4} (\phi_{i+1,j+1} - \phi_{i+1,j-1} - \phi_{i-1,j+1} + \phi_{i-1,j-1}) \\ \Delta^{jj} \phi_{i,j} &= \phi_{i,j+1} - 2\phi_{i,j} + \phi_{i,j-1} \end{aligned}$$

In this case, we have the following update equation:

$$\begin{aligned} \frac{\phi_{i,j}^{n+1} - \phi_{i,j}^n}{\Delta t} &= [\beta k_{i,j}^n - \text{dist}^2(T_{i,j}, T_1^n) + \text{dist}^2(T_{i,j}, T_2^n)] \sqrt{(\Delta^i \phi_{i,j})^2 + (\Delta^j \phi_{i,j})^2} \\ T_1^n &= \frac{\sum_{i,j} (1 - H(\phi_{i,j}^n)) T_{i,j}}{\sum_{i,j} (1 - H(\phi_{i,j}^n))}, \quad T_2^n = \frac{\sum_{i,j} H(\phi_{i,j}^n) T_{i,j}}{\sum_{i,j} H(\phi_{i,j}^n)} \end{aligned} \quad (7)$$

where the curvature $k_{i,j}^n$ of ϕ^n can be computed as:

$$k_{i,j}^n = \frac{\Delta^{jj} \phi_{i,j}^n (\Delta^i \phi_{i,j}^n)^2 - 2\Delta^i \phi_{i,j}^n \Delta^j \phi_{i,j}^n \Delta^{ij} \phi_{i,j}^n + \Delta^{ii} \phi_{i,j}^n (\Delta^j \phi_{i,j}^n)^2}{[(\Delta^i \phi_{i,j}^n)^2 + (\Delta^j \phi_{i,j}^n)^2]^{3/2}} \quad (8)$$

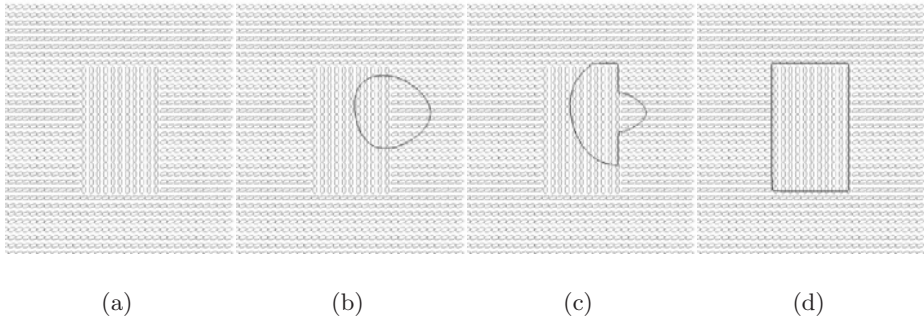


Fig. 1. Segmentation of a synthetic tensor field where two regions differs only in the orientations, (b),(c) and (d) are the initial, intermediate and final steps of the curve evolution process in the segmentation.

There are many other efficient numerical schemes that one may employ for example the multigrid scheme as was done in Tsai et.al., [17]. At this time, our explicit Euler scheme yielded reasonably fast solutions (3-5secs. for the synthetic data examples and just under a minute for the real data examples on a 1Ghz Pentium-3 CPU). For the piecewise smooth model, we refer the readers to ([8], [17]) for implementation details.

4 Experimental Results

In this section, we present several sets of experiments on the application of our tensor field segmentation model. One is on 2D synthetic data sets, the second is on texture images, the third one and the last one are on slices of diffusion tensor fields estimated from diffusion weighted images. We apply the piecewise constant case of our model for the first three sets of examples and the original piecewise smooth model for the last example. In all examples, the evolving boundary of the segmentation are superimposed on the images either in black or white.

4.1 Synthetic Tensor Field Segmentation

We synthesize two tensor fields, both are 2×2 symmetric positive definite matrix valued images on a 128×128 lattice and have two homogeneous regions. The two regions in the first tensor field only differ in the orientations while the two regions in the second tensor field only differ in the scales. These two tensor fields are visualized by ellipses as shown in Figure 1(a) and Figure 2(a). With an arbitrary initialization of the geometric active contour, our proposed model can yield high quality segmentation results as show in Figure 1 and Figure 2. Note that the first tensor field can't be segmented by using scalar anisotropic properties of tensors as in [18] and the second tensor field can't be segmented by using the dominant eigen vectors of the tensors. These two examples show that one must use the full information contained in tensors.

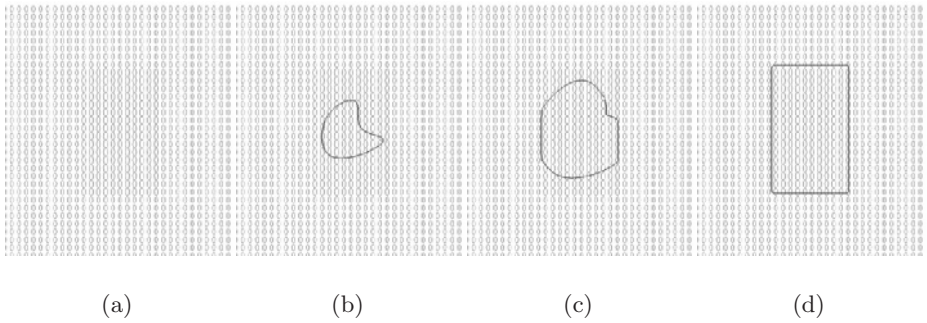


Fig. 2. Segmentation of a synthetic tensor field where two regions differs only in the scales, (b), (c) and (d) are the initial, intermediate and final steps of the curve evolution process in the segmentation.

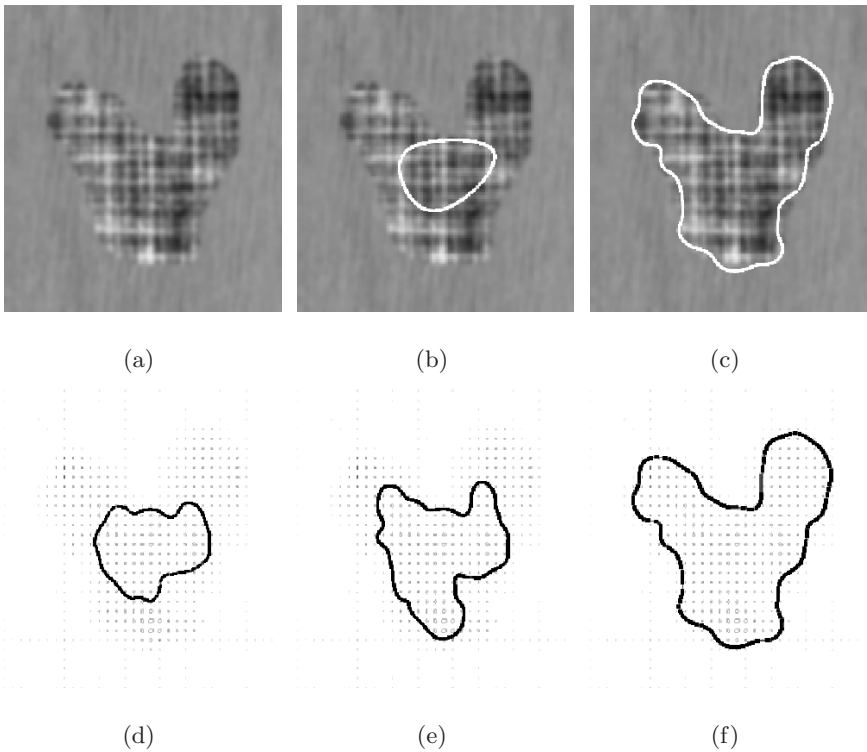


Fig. 3. Texture segmentation for a heart shape region: (b) and (c) are the initial and final curve superimposed on the texture image. (d), (e) and (f) are the intermediate and final steps with the evolving curve superimposed on the structure tensor field.

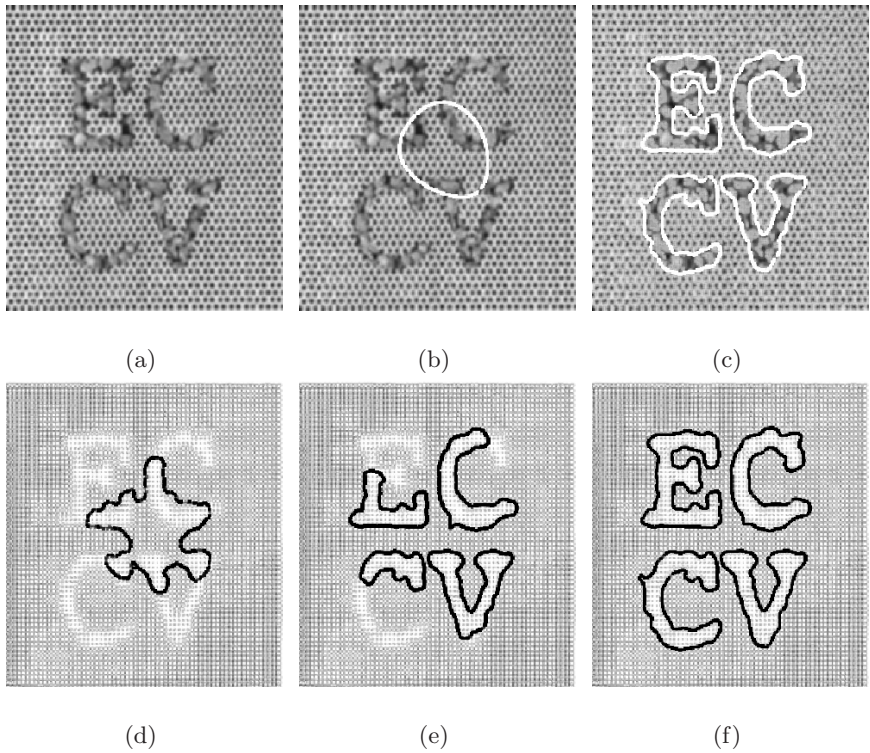


Fig. 4. Texture segmentation for a region showing "ECCV" logo: (b) and (c) are the initial and final curve superimposed on the texture image. (d),(e) and (f) are the intermediate and final steps with the evolving curve superimposed on the structure tensor field.

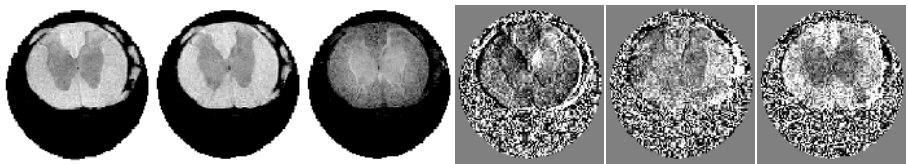


Fig. 5. A slice of the diffusion tensor field of a normal rat spinal cord. Each component is shown as a scalar image. Left to right : D_{xx} , D_{yy} , D_{zz} , D_{xy} , D_{yz} and D_{xz} respectively, the offdiagonal terms D_{xy} , D_{yz} and D_{zz} are greatly enhanced by brightness and contrast changes for better visualization.

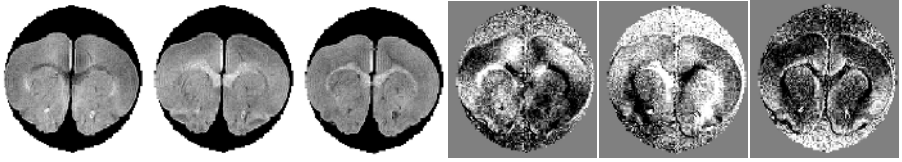


Fig. 6. A slice of the diffusion tensor field of a normal rat brain. Each component is shown as a scalar image. Left to right : D_{xx} , D_{yy} , D_{zz} , D_{xy} , D_{yz} and D_{xz} respectively, the offdiagonal terms D_{xy} , D_{yz} and D_{xz} are greatly enhanced by brightness and contrast changes for better visualization.

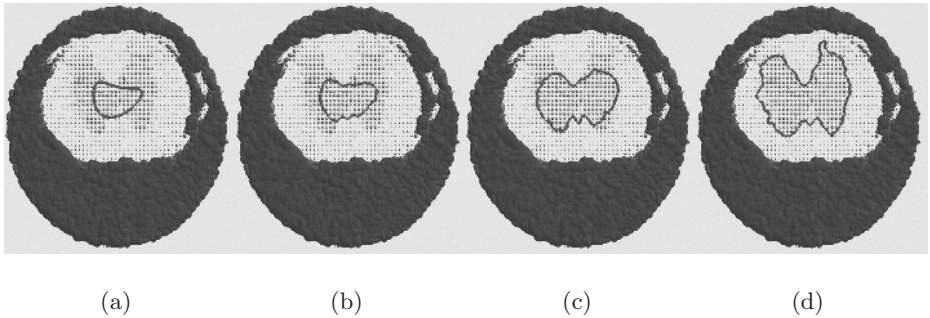


Fig. 7. Segmentation of the slice of the diffusion tensor image shown in figure (5). (a)-(d) are the initial, intermediate and final steps of the curve evolution process in segmenting the gray matter inside the spinal cord.

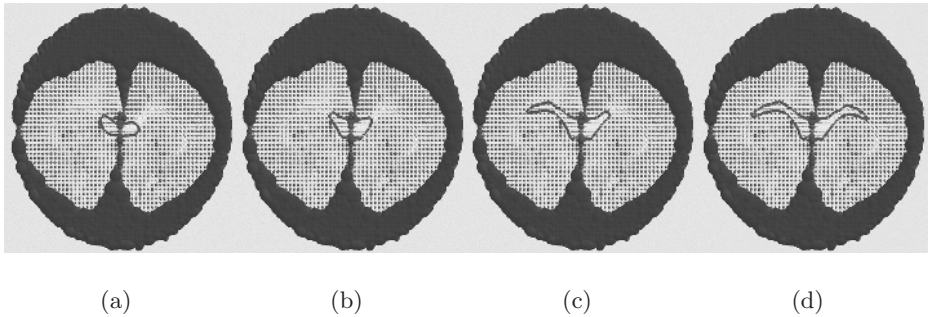


Fig. 8. Segmentation of the slice of the diffusion tensor image shown in figure (6). (a)-(d) are the initial, intermediate and final steps of the curve evolution process in segmenting the corpus callosum inside the rat brain.

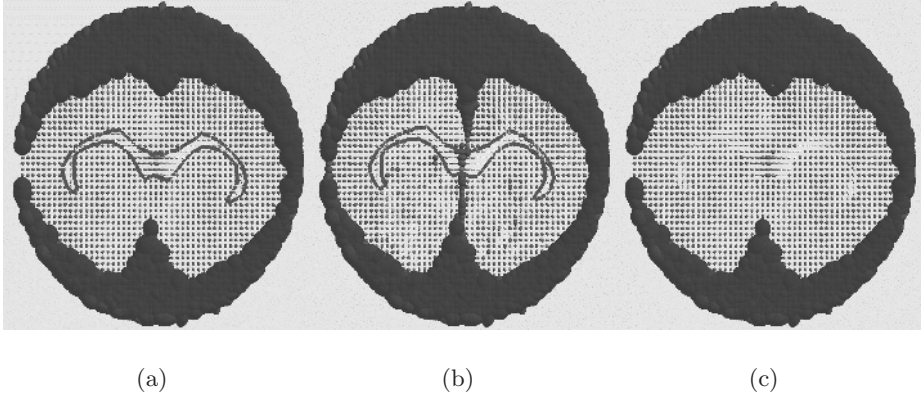


Fig. 9. Use piecewise smooth model to segment the slice of the diffusion tensor image shown in figure (6). (a) and (b) show the boundary of the final segmentation superimposed on the smoothed and the original tensor field respectively. (c) is the smoothed tensor field.

4.2 Texture Image Segmentation

For texture image segmentation, we construct the structure tensor field from the given image and then segment the structure tensor field using our proposed model. The structure tensor is defined as [3]:

$$J_\rho = K_\rho * (\nabla I \nabla I^T)$$

where K_ρ is a Gaussian smoothing function with standard deviation ρ . Figures 3 and 4 respectively show that our method can yield reasonable quality texture segmentations. Note that the segmentations are not very accurate along the edges of the original texture images. This is because we did not use any anisotropic smoothing for the structure tensor field as in [16], thus the edges in the original image were not preserved. It is however easy to incorporate such an anisotropic smoothing to yield better quality segmentations and will be the focus of our future work. Figure 4 also shows that topological change of the regions can be achieved easily in a level set framework.

4.3 Diffusion Tensor Image Segmentation

Diffusion tensor MRI (DT-MRI) is a relatively new MR imaging modality from which anisotropy of water diffusion can be inferred quantitatively [2], thus providing a method to study the tissue microstructure e.g., white matter connectivity in the brain in vivo. Diffusion is a process of movement of molecules as a result of random thermal agitation and in DT-MRI context, refers specifically to the random translational motion of water molecules in the part of the anatomy being imaged with MR. In three dimension, water diffusivity can be described by a 3×3 symmetric positive definite matrix \mathbf{D} called diffusion tensor

which is intimately related to the geometry and organization of the microscopic environment.

In DT-MRI, what is measured is the diffusion weighted echo intensity image (DWI) S_l . They are related to the diffusion tensor \mathbf{D} through the Stejskal-Tanner equation [2] as given by:

$$S_l = S_0 e^{-\mathbf{b}_l \cdot \mathbf{D}} = S_0 e^{-\sum_{i=1}^3 \sum_{j=1}^3 b_{l,ij} D_{ij}} \quad (9)$$

where \mathbf{b}_l is the diffusion weighting of the l -th magnetic gradient, “ \cdot ” denotes the generalized inner product for matrices. Given several non-collinear diffusion weighted intensity measurements, \mathbf{D} can be estimated via multivariate regression models.

Figure 5 shows a slice of the diffusion tensor field estimated from the DWIs of a normal rat spinal cord and Figure 6 shows the same for a normal rat brain. Each of the six independent components of the individual symmetric positive definite diffusion tensors in the tensor field is shown as a scalar image. Figure 7 demonstrates the segmentation of the gray matter inside the normal rat spinal cord with the evolving curve superimposed on the ellipsoid visualization of the diffusion tensor field. Similarly, Figure 8 depicts the segmentation procedure for the normal rat brain. In the final step, the major part of the corpus callosum is captured by the piecewise constant segmentation model. In both cases, we exclude the free water region which is not of interest in a biological context.

4.4 DTI Segmentation Using the Piecewise Smooth Model

Most of the previous examples have been successfully segmented using the piecewise constant model, however with one exception as shown in Figure 8 because the piecewise constant assumption is no longer valid. Thus we further employ the piecewise smooth model to refine the segmentation result in Figure 8 and show the result of this application in Figure 9. Note that the horns of the corpus callosum have been accurately captured using the piecewise smooth model unlike when using the piecewise constant region model used in Figure 8.

5 Conclusion

We presented a tensor field segmentation method by incorporating a discriminant for tensors into a region-based active contour model. The particular discriminant we employed is the Euclidean difference measure between tensors. By using a discriminant on tensors, as opposed to either the eigen values or the eigen vectors of the tensors, we make full use of all the information contained in tensors. This proposed model is then implemented in a level set framework to take advantage of the easy ability of this framework to change topologies when desired. Our approach was applied to 2D synthetic and diffusion tensor field segmentation as well as texture image segmentation by using its structure tensor field. The experimental results are very good, essential part of the regions are well captured and topological changes are handled naturally.

The given model here can be further improved in many ways. Our future work will include the following: (i) a better discriminant of tensors needs to be used. Though the Euclidean difference measure use the full tensor information, it blindly uses the same weights for different components of the tensor and ignores the fact that tensors have structure. (ii) shape statistics can be incorporated to improve the robustness and accuracy of the current model.

Acknowledgment. We thank Dr. T. Mareci and E. Özarlan for providing the DT-MRI data and Dr. R. Deriche for his valuable comments on this research.

References

1. D. Alexander, J.C. Gee, and R. Bajcsy. Similarity measure for matching diffusion tensor images. In *British Machine Vision Conference*, pages 93–102, University of Nottingham, Sept. 1999.
2. P. J. Basser, J. Mattiello, and D. Lebihan. Estimation of the effective self-diffusion tensor from the nmr spin echo. *Journal of Magnetic Resonance*, (103):247–254, 1994.
3. Jähne Bernd. *Digital Image Processing: Concepts, Algorithms, and Scientific Applications with CDROM*. Springer-Verlag Telos, 2001.
4. J. Bigün, G. H. Granlund, and J. Wiklund. Multidimensional orientation estimation with applications to texture analysis and optical flow. *IEEE Trans. on Pattern Analysis and Machine Intelligence*, 13(2):775–790, 1991.
5. V. Caselles, F. Catte, T. Coll, and F. Dibos. A geometric model for active contours in image processing. *Numerische Mathematik*, 66:1–31, 1993.
6. V. Caselles, R. Kimmel, and G. Sapiro. Geodesic active contours. In *Fifth International Conference on Computer Vision*, pages 694–699, 1995.
7. T. F. Chan and L. A. Vese. Active contours without edges. *IEEE Trans. on Image Processing*, 10(2):266–277, Feb. 2001.
8. T. F. Chan and L. A. Vese. A level set algorithm for minimizing the mumford-shah functional in image processing. In *IEEE Workshop on Variational and Level Set Methods*, pages 161–168, 2001.
9. H. Haußecker and B. Jähne. A tensor approach for precise computation of dense displacement vector fields. In *Proc. Mustererkennung*, Berlin, German, 1997.
10. S. Kichenassamy, A. Kumar, P. Olver, A. Tannenbaum, and A. Yezzi. Gradient flows and geometric active contour models. In *Fifth International Conference on Computer Vision*, Cambridge, MA, 1995.
11. G. Kühne, J. Weickert, O. Schuster, and S. Richter. A tensor-driven active contour model for moving object segmentation. In *IEEE International Conference on Image Processing*, pages 73–76, Thessaloniki, Greece, Oct. 2001.
12. T. Brox M. Rousson and R. Deriche. Active unsupervised texture segmentation on a diffusion based feature space non-rigid registration. In *IEEE Conference on Computer Vision and Pattern Recognition*, Wisconsin, USA, June 2003.
13. R. Malladi, J. A. Sethian, and B. C. Vemuri. A topology independent shape modeling scheme. In *SPIE Proc. on Geometric Methods in Computer Vision II*, volume 2031, pages 246–256,. SPIE, July 1993,.
14. R. Malladi, J. A. Sethian, and B. C. Vemuri. Shape modeling with front propagation : A level set approach. *IEEE Trans. Pattern Analysis and Machine Intelligence*, 17(2):158–175, 1995.

15. D. Mumford and J. Shah. Optimal approximations by piecewise smooth functions and associated variational-problems. *Communications on Pure and Applied Mathematics*, 42:577–685, 1989.
16. M. Rousson, T. Brox, and R. Deriche. Active unsupervised texture segmentation on a diffusion based feature space. Technical Report RR-4695, INRIA, France, Jan. 2003.
17. A. Tsai, Jr. A. Yezzi, and A. S. Willsky. Curve evolution implementation of the mumford-shah functional for image segmentation, denoising, interpolation, and magnification. *IEEE Trans. on Image Processing*, 10(8):1169–1186, Aug. 2001.
18. L. Zhukov, K. Museth, D. Breen, R. Whitaker, and A. Barr. Level set modeling and segmentation of dt-mri brain data. *Journal of Electronic Imaging*, 12(1):125–133, Jan. 2003.